Unravelling dislocation networks in metals

Arechabaleta Guenechea, Zaloa; van Liempt, Peter; Sietsma, Jilt

DOI
10.1016/j.msea.2017.10.099

Publication date
2018

Document Version
Final published version

Published in
Materials Science and Engineering A: Structural Materials: Properties, Microstructures and Processing

Materials Science & Engineering A 710 (2018) 329–333

Contents lists available at ScienceDirect

Materials Science & Engineering A

journal homepage: www.elsevier.com/locate/msea

Unravelling dislocation networks in metals

Zaloa Arechabaleta*, Peter van Liempt, Jilt Sietsma

Dept. Materials Science and Engineering, Delft University of Technology, Mekelweg 2, 2628 CD Delft, The Netherlands

ARTICLE INFO

Keywords:
Anelastic strain
Dislocation network
Yield stress
Taylor equation

ABSTRACT

Understanding the intricate structure of dislocations in metals is a major issue in materials science. In this paper we present a comprehensive approach for the characterisation of dislocation networks, resulting in accurate quantification and significantly increasing the insight into the dislocation structure. Dislocation networks in metals consists of dislocation segments, pinned by microstructural obstacles. In the present paper a model is introduced that describes the behaviour of these dislocation segments in the pre-yield range of a tensile test on the basis of fundamental concepts of dislocation theory. The model enables experimental quantification of the dislocation density and segment length from the tensile curve. Quantitative results are shown and discussed on the development of the dislocation network as a function of increasing degree of plastic deformation, including validation and physical interpretation of the classical Taylor equation.

1. Introduction

The mechanical behaviour of metals is governed by dislocations. Dislocation lines, spontaneously occurring lattice defects, are present in any crystalline metal at a typical density ρ of 10^{11}–10^{15} metre per cubic metre material (m^{-2}). It is generally accepted that their motion effectuates plastic deformation. In most models for dislocation behaviour "a dislocation" is considered as a discrete entity, which either remains stationary or becomes mobile when subjected to a mechanical stress [1]. These distinct dislocations are envisaged to interact through their surrounding strain fields. However, dislocations cannot end within a crystalline structure [2] and they can therefore not be regarded as discrete, separate units. *Dislocations form a continuous network*. This network, termed "Frank net" by Cottrell in 1957 [3], interacts with microstructural features like precipitates, solute atoms and grain boundaries and self-interacts with dislocation lines within the network (see Fig. 1a). In the interaction points, dislocation motion is impeded and these points are commonly indicated as "pinning points". The network is thus subdivided into dislocation segments between microstructural pinning points. When applying a stress, the central parts of the segments can and will move, but the segments do remain attached to the pinning points. The motion of dislocations thus consists of the bowing out of dislocation segments (a schematic example is given for one segment in Fig. 1a). The main characteristics of the dislocation network that are relevant for the strength and deformation of the metal are the dislocation density and the distribution of dislocation segment lengths. The present paper will show that these characteristics can be quantitatively determined from a repeated cycling tensile test (see Fig. 1b and c for the equipment and results on a low-alloy (LA) and an interstitial-free (IF) steel studied in this paper), an experimental method that is easily and cheaply accessible for every materials scientist.

2. Experimental

Repeated cycling tensile tests were performed on two samples of the LA steel and two samples of the IF steel. Both are single-phase ferritic (BCC) steels. The main alloying elements for the LA steel are 0.08 wt% C, 0.30 wt% Mn, 0.10 wt% Si, and for the IF steel 47 wt-ppm C, 0.15 wt% Mn, 0.049 wt% Ti. The tensile tests were conducted on an Instron 5982 electromechanical tester, with a maximum capacity of 100 kN, at room temperature and in displacement control. Standard ASTME E-8 dog-bone specimens of 1.0 mm thickness were used for the LA steel, whereas for the IF steel the dog-bone specimens were of 275 mm total length, 60 mm gauge length and 12.5 mm gauge width, with a thickness of 0.7 mm. In order to accurately measure the strain, also at small strain in the pre-yield region, a duplex extensometer set-up was used (Fig. 1b) [4]. The repeated cycling tests consisted of 20 loading and unloading steps, in each of which the stress was reduced to 10 MPa after the application of 0.5% plastic true strain.

3. Results and discussion

The cycling true stress-strain curves, averaged over the two measurements for each steel grade, are shown in Fig. 1c. The first loading

* Corresponding author.
E-mail address: z.arechabaletaguenechea@tudelft.nl (Z. Arechabaleta).

http://dx.doi.org/10.1016/j.msea.2017.10.099
Received 7 August 2017; Accepted 27 October 2017
Available online 28 October 2017

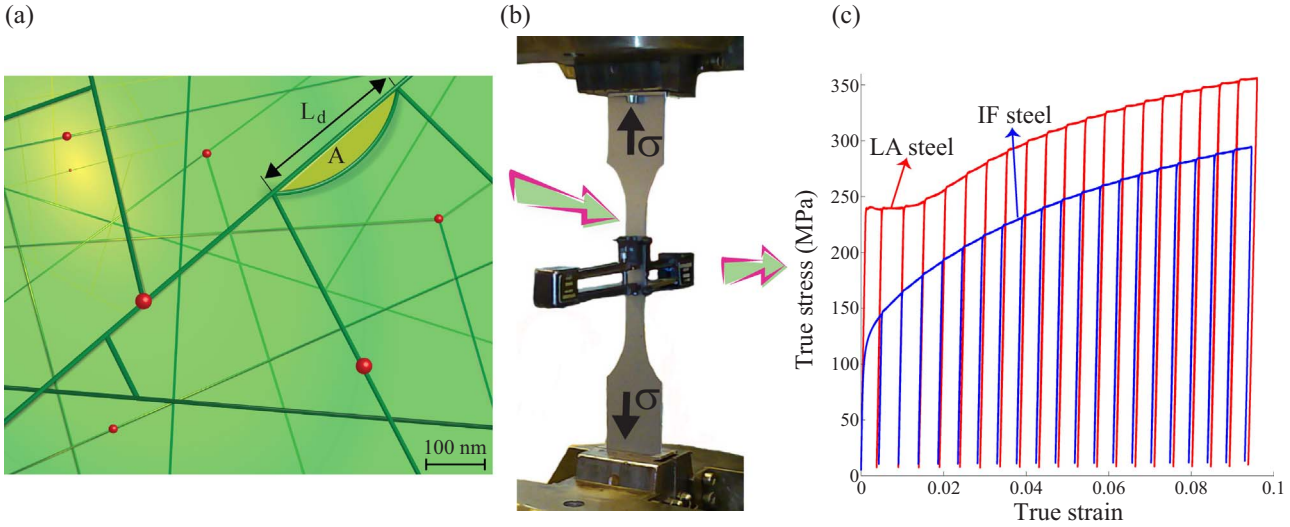

Fig. 1. The mechanical behaviour of metals during a tensile test. (a) Schematic representation of the dislocation network, with segments terminating at self-interaction points of the network, at average distance L_d, and at microstructural pinning points caused by other obstacles, like precipitates, jogs, solute atoms and grain boundaries (red dots). At zero stress, all segments are straight; the bowing out of dislocation segments, sweeping an area A when a small stress is applied, is shown for one segment. The scale bar is merely indicative. (b) The tensile test, with the duplex extensometer set-up [4]. (c) The repeated cycling tensile curves for the Low-Alloy (LA) and the Interstitial-Free (IF) steels that were investigated in this study.

step was not included in the analysis, because it was affected by internal stresses and imperfect initial alignment of the samples. The Low-Alloy steel shows the phenomenon of yield point extension and therefore also the second and third cycle of this steel were not included in the analysis. Each loading curve consists of a pre-yield region with subsequently a transition to plastic deformation at the stress that is indicated as the yield stress in the present paper. This quantity is also often indicated as the flow stress, but in these experiments it is actually the stress at which yielding (re)occurs, which is why we will refer to this quantity as the yield stress. From Fig. 1c it can readily be seen that the yield stress in the subsequent loading steps depends on the plastic strain ε_p. This dependence, the work hardening behaviour, is generally known to be caused by the development of the dislocation structure within the metal during plastic deformation. Understanding the dislocation structure in metals is therefore of paramount importance for understanding the mechanical behaviour of these materials. Nevertheless, in most experimental and modelling studies the intricate dislocation structure is characterised by just one parameter, the dislocation density ρ. Moreover, the experimental determination of the dislocation density is complicated and can be achieved only with limited accuracy. Transmission Electron Microscopy can be used for direct observation of dislocations, but effects of sample preparation and the limited volume that can be probed do not allow accurate quantification [3]. X-Ray Diffraction is commonly employed for experimental determination of the dislocation density [5–7], but the quantification requires restrictive assumptions in the analysis that cannot be independently tested and that render quantification on an absolute scale cumbersome. Nevertheless, X-Ray diffraction has been employed in many experimental studies to determine the dislocation density [4,8,9], including in situ studies by synchrotron radiation [10,11]. The electrical resistivity has also been proposed for the experimental determination of ρ [12], but this is an indirect method that requires additional assumptions. However, basic dislocation theory shows that it is not in the first place the dislocation density, but the length of dislocation segments that governs the mechanical behaviour of metals. Therefore a scientific focus on dislocation segment-length distribution is crucial for a better understanding of the mechanical behaviour of crystalline metals. Regrettably, very limited experimental information on dislocation segment lengths is available in the literature. Jakobsen et al. [13] have presented synchrotron observations on the localised behaviour of dislocations. Messerschmidt [14] discusses internal friction measurements for the analysis of the dislocation segment length, but application of the method has been very limited. To the best of the authors' knowledge no method is available with which a quantitative overall picture of dislocation segments in a metal can be obtained. The present paper will show that such quantification is possible by analysing the pre-yield behaviour during a tensile test.

Classical dislocation theory describing the behaviour of a dislocation segment that is bowing out under the influence of a mechanical stress (Fig. 1a) is widely accepted [3]. The central equation gives the relation between an applied stress σ and the radius of curvature r of the bowing dislocation segment, a consequence of the dislocation line stress being in equilibrium with the applied stress:

$$\sigma = \frac{MGb}{2r}, \tag{1}$$

in which M is the Taylor factor, G the shear modulus and b the length of the Burgers vector [15]. The bowing out of a dislocation segment of length L becomes critical at a stress σ_c given by

$$\sigma_c = \frac{MGb}{L}. \tag{2}$$

At stresses higher than σ_c the dislocation line stress can no longer compensate the applied stress, the stress equilibrium is lost and the dislocation segment is activated as a Frank-Read source. This is the onset of plastic deformation and σ_c is therefore the stress at which the dislocation segment of length L yields. Considering the entire structure, a distribution of segment lengths will be present. The macroscopically observed yield stress σ_y is determined by an effective segment length representing this distribution. We assume that this effective length can be approximated by the average segment length $\overline{L}$, which is then related to σ_y by an equation that is equivalent to Eq. (2):

$$\sigma_y = \frac{\overline{M}Gb}{\overline{L}}, \tag{3}$$

involving the average Taylor factor $\overline{M}$ ($\overline{M}$ = 3.06 for BCC [16]). Note that $\overline{L}$ is not determined by the distances between self-interaction points of the dislocation network only (Fig. 1a), because of the influence of other microstructural pinning points, like solute atoms and precipitates. These points include grain boundaries, so the grain size effect on the yield stress is also effectuated in $\overline{L}$.

At the start of the tensile test, when the applied stress is zero, the dislocation segments are in principle straight between their pinning

points, which is the configuration with the lowest defect energy because of the minimum length of the dislocation lines. At a non-zero stress below the yield stress, i.e. in the pre-yield region, each dislocation segment will bow out to a certain extent, into a circle segment [3], schematically shown for one segment in Fig. 1a. The extent of bowing is determined by the equilibrium between applied stress and dislocation line stress, as described by Eq. (1). Note that this process does not induce any irreversible change in the dislocation network. The bowing out of N dislocation segments per cubic metre causes an equivalent true strain ε_a that is reversible in nature and is called anelastic strain [4,17]. A dislocation network of N segments of average length $\overline{L}$ represents a dislocation density $\rho = N\overline{L}$. The anelastic strain is then given by

$$\varepsilon_a = \frac{Nb\overline{A}}{\overline{M}} = \frac{\rho b\overline{A}}{\overline{M}\overline{L}}, \tag{4}$$

where $\overline{A}$ is the average area swept by the dislocations in moving from the straight zero-stress configuration to the curved configuration (see Fig. 1a). The anelastic strain is additional to the lattice strain σ/E that is determined by the Young's modulus E, and thus causes a decrease of the apparent Young's modulus $\Theta = \frac{d\sigma}{d\varepsilon}$. Eq. (4) shows that the pre-yield region of the tensile curve contains information on the dislocation density ρ and the average segment length $\overline{L}$. This information can be extracted when considering the extended Kocks-Mecking (KM) plot [4,17], a plot of Θ as a function of σ.

In Fig. 2 several examples are given of extended Kocks-Mecking plots for the loading steps in the tensile curves in Fig. 1c. Fig. 2 shows the distinct deviation of Θ from the value of the Young's modulus, which is caused by additional anelastic strain due to the bowing out of dislocations (Eq. (4)). The plastic region of the extended KM-plot (Fig. 2) is barely visible because of the small values of both Θ and the stress increase in this region as compared to the (an)elastic region. At very low values of σ, Θ is influenced by effects of the preceding unloading step, as will be discussed in a forthcoming paper on the unloading behaviour of the dislocation network.

	Cycle 3	Cycle 10	Cycle 17
True plastic strain (ε_p)	0.009	0.042	0.075
ρ (m^{-2})	1.6 x 10^{13}	4.5 x 10^{13}	6.8 x 10^{13}
$\overline{L}$ (nm)	375	258	221
σ_y (MPa)	165	240	280

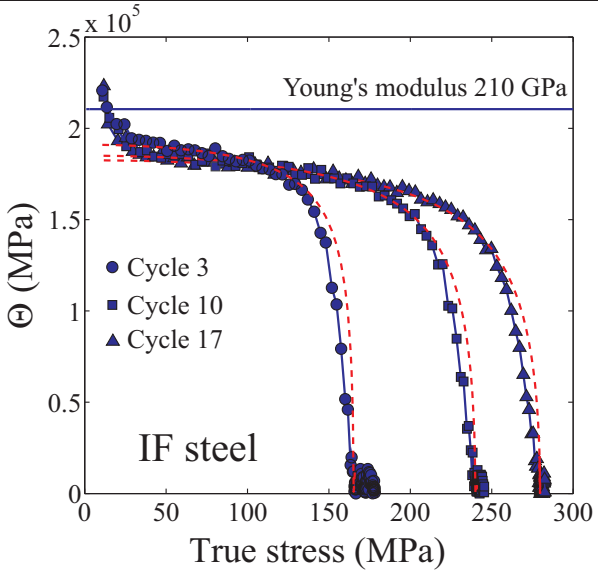

Fig. 2. The extended Kocks-Mecking plot for the loading steps 3, 10 and 17 of the IF steel. The dashed red lines give the model description by Eq. (5), from which the dislocation density, the average segment length and the yield stress are derived. The values are given in the table at the top of the figure. Some disagreement between model and experiment is observed at low stress, due to effects of the preceding unloading step, and at stresses approaching the yield stress, most likely due to microplasticity.

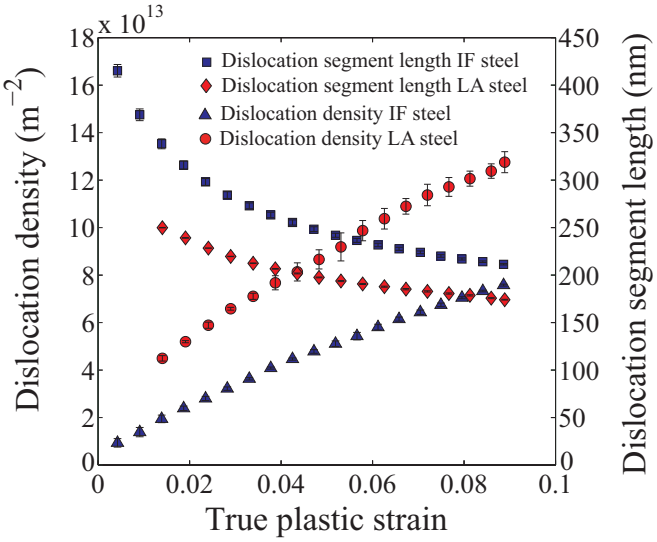

Fig. 3. The average segment length and the dislocation density as a function of the applied plastic strain, derived from the extended Kocks-Mecking plots of the loading steps, fitted with Eq. (5), for which examples have been given in Fig. 2. The experimental uncertainties, evaluated on the basis of Eq. (5), are indicated by the error bars, most of which are smaller than the symbols.

As early as 1956, the initial value for Θ, at $\sigma = 0$, was related, starting from Eq. (4), to the quantity $\rho\overline{L}^2$ by Schoeck [18], but recently Van Liempt and Sietsma derived, based on the same physical principles, the equation that describes the entire pre-yield part of the extended Kocks-Mecking plot [17]:

$$\Theta = \frac{\overline{M}^2 E s^3\sqrt{1-s^2}}{\overline{M}^2 s^3\sqrt{1-s^2} + \rho\overline{L}^2(1+\nu)(s - \sqrt{(1-s^2)}\arcsin(s))}, \tag{5}$$

with $s = \sigma/\sigma_y$ and ν is Poisson's ratio ($\nu = 0.29$). The red dashed lines in Fig. 2 show the fits of this equation to the pre-yield region of several loading curves. The agreement is seen to be very good, except for the aforementioned spurious effect of the preceding unloading step at low σ and the somewhat lower experimental Θ-values at higher σ, most likely caused by microplasticity. The fit of Eq. (5) eventually involves two fitting parameters: the dislocation density ρ and the average segment length $\overline{L}$. The latter determines the value of σ_y, and thus s, through Eq. (3).

The evolution of the dislocation density ρ and the average segment length $\overline{L}$ as a function of plastic strain ε_p, is shown in Fig. 3 for both steel grades. The pre-yield region of the tensile curve is thus shown to supply quantitative information on the dislocation network, developing as a function of plastic strain.

The decrease of the average dislocation segment length, related to the increase in dislocation density, causes the material to become stronger, a phenomenon that is known as work hardening. It has since long been accepted that the so-called Taylor equation [19] describes the relation between yield stress and dislocation density. This equation reads:

$$\sigma_y = \sigma_0 + \alpha\overline{M}Gb\sqrt{\rho}. \tag{6}$$

In this equation α is a constant, for which usually values in the range 0.15–0.4 are assumed. The first term in this equation, σ_0, represents the strength contribution due to other microstructural obstacles than dislocations. The Taylor equation is based on considering dislocations as separate entities, which interact through the strain fields surrounding them. The distance between these dislocations is assumed to be inversely proportional to $\sqrt{\rho}$, while the character of α is not clearly defined. Although widely accepted, the Taylor equation should be considered as a semi-empirical relation, where its validation is very limited due to the poor accuracy of dislocation density data and to the

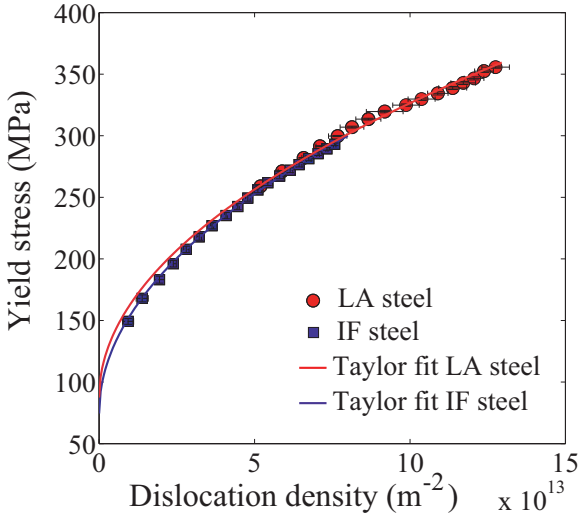

Fig. 4. Experimental validation of the Taylor equation (Eq. (6)) for the two steels investigated in the present study. The experimental uncertainty in the yield stress, evaluated on the basis of the Eqs. (5) and (3), is smaller than the symbols.

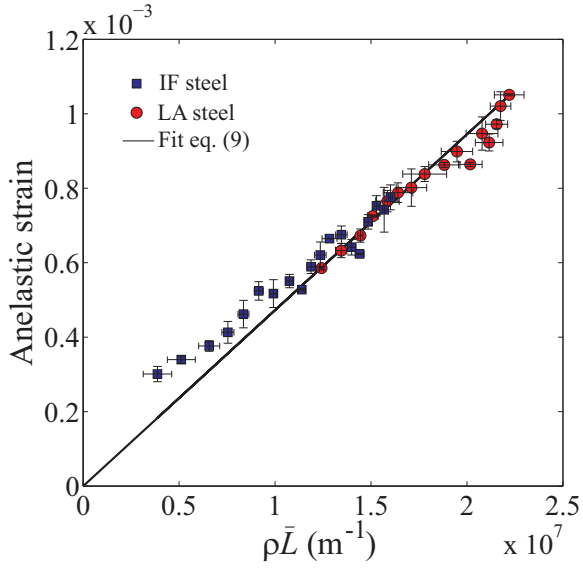

Fig. 5. The relation between the anelastic strain at the yield stress and the characteristics ρ and $\bar{L}$ of the dislocation network. The solid line shows the linear relation expressed by Eq. (9).

experimental ambiguity in the determination of the yield stress, in which the widely applied 0.2% offset method is practically useful, but it is not based on the dislocation behaviour. Moreover, no physical meaning has yet been proposed for the parameter α. The measurements presented in the present paper provide a possibility for experimental validation of the Taylor equation. The relation between the yield stress and the dislocation density and the fit to Eq. (6) is shown in Fig. 4 for both materials. It can be seen that the fit of the Taylor equation is very accurate, yielding the values $\sigma_0 = (87 \pm 5)$ MPa and $\sigma_0 = (84 \pm 5)$ MPa for the LA steel and the IF steel, respectively. For the parameter α, the value $\alpha = 0.389 \pm 0.010$ is found for the LA steel and $\alpha = 0.410 \pm 0.010$ for the IF steel.

The validity of the Taylor equation allows for further analysis of the dislocation network. The second term in the Taylor equation represents the strength contribution σ_d (equal to $\sigma_y - \sigma_0$) that is due to pinning by self-interaction points of the dislocation network, with average distance $\bar{L}_d$ (see Fig. 1a). Now that the value of σ_0 has been determined (Fig. 4), for each loading cycle the distance $\bar{L}_d$, representative for the dislocation network (Fig. 1a), can be calculated by means of

$$\sigma_d = \alpha \bar{M} G b \sqrt{\rho} = \frac{\bar{M} G b}{\bar{L}_d}. \tag{7}$$

Eq. (7) shows the physical meaning of the Taylor parameter α in the present interpretation of the dislocation behaviour:

$$\alpha = (\bar{L}_d \sqrt{\rho})^{-1}. \tag{8}$$

The parameter α thus relates the observable parameter, the dislocation density, with the microstructural parameter that determines yielding, the segment length. The dimensionless quantity $\bar{L}_d \sqrt{\rho}$ represents the structure of the dislocation network, combining its characteristics ρ and $\bar{L}_d$. The validation of the Taylor equation (Fig. 4) implies that the parameter α retains a constant value when the dislocation network changes as a consequence of the plastic deformation process. This implies that the quantity $\bar{L}_d \sqrt{\rho}$, a quantitative representation of the dislocation network, remains constant (having the values 2.58 ± 0.07 for the LA steel and 2.44 ± 0.06 for the IF steel), although ρ changes. Such observations enable closer studies of the processes that lead to the evolution of the dislocation network during plastic deformation.

The novel approach presented in this study to come to better understanding of the role of the dislocation network in plastic deformation of metals yields an accurate and consistent quantification of dislocation characteristics, derived from the pre-yield part of the tensile curve. The consistency of the approach and the resulting values can further be examined by considering the magnitude of the anelastic strain that results from dislocations bowing out in the pre-yield region ε_a, Eq. (4). When the applied stress is approaching the yield stress, the dislocation segments evolve towards semi-circles. At the yield stress, when a dislocation segment has become a semi-circle, it has swept an area $\frac{\pi}{8}\bar{L}^2$. Inserting the average value $\frac{\pi}{8}\bar{L}^2$ for $\bar{A}$ into Eq. (4), the average anelastic strain at the yield stress, ε_a^y, can be expressed as

$$\varepsilon_a^y = \frac{\pi b \rho \bar{L}^2}{8\bar{M}\bar{L}} = \left(1 + \frac{\sigma_L^2}{\bar{L}^2}\right)\frac{\pi b}{8\bar{M}}\rho\bar{L}, \tag{9}$$

with $\sigma_L^2 = \overline{L^2} - \bar{L}^2$ the variance of the segment length distribution. The magnitude of the anelastic strain is not only of theoretical interest, but also at the basis of the magnitude of springback, a technologically important phenomenon. In the present study, the anelastic strain at the yield stress has been experimentally determined from each loading curve by subtracting the elastic strain σ_y/E from the total strain at $\sigma = \sigma_y$. Its relation with the product $\rho\bar{L}$ is shown in Fig. 5. The figure shows that indeed a linear relation is found, albeit with a slight deviation at low values of $\rho\bar{L}$. The slope of the line fitted with Eq. (9) is (0.047 ± 0.002) nm for the two steels. This implies, using the previously given values for b and $\bar{M}$, $\sigma_L^2 \approx 0.5\bar{L}^2$. This analysis of the anelastic strain again shows the consistency of the present approach and provides information on the width of the distribution of segment lengths in the dislocation network.

4. Conclusions

The present study proposes an accessible, cheap and accurate method to quantify the dislocation network in metals, based on tensile tests and widely accepted physical principles of dislocation behaviour. Besides the quantification of the dislocation density, the method also yields the value of the average dislocation segment length and even an estimate of the width of the segment length distribution. An accurate experimental validation of the Taylor equation for work hardening is presented, introducing the physical meaning of the parameter α in this equation (Eq. (8)). Wider application of this method can lead to valuable increased insight into the behaviour of dislocations in many aspects, like the effect of bake hardening in steel due to the decrease of the segment length while the dislocation network remains unaffected,

the magnitude of springback that is directly related to the density and behaviour of dislocations during unloading, the interaction between dislocations and precipitates, the mechanisms of recovery and many other examples.

Acknowledgements

This research was supported by the Dutch Technology Foundation (STW) and carried out under the project number S22.1.13494b in the framework of the Research Programme of the Materials innovation institute (M2i) (www.m2i.nl). The support of M2i and Tata Steel RD & T is gratefully acknowledged. The authors wish to thank the Thermoplastic Composites Research Center (TPRC) at Twente University in the Netherlands for the support in the mechanical tests and Richard Huizenga for discussions and help in preparing Fig. 1.

References

[1] E. van der Giessen, A. Needleman, A discrete dislocation plasticity: a simple planar model, Model. Simul. Mater. Sci. Eng. 3 (1995) 689–735.
[2] F.R.N. Nabarro, Theory of Crystal Dislocations, Clarendon Press, Oxford, 1967.
[3] D. Hull, D.J. Bacon, Introduction to Dislocations, 5th ed., Elsevier, Oxford, 2011.
[4] Z. Arechabaleta, P. van Liempt, J. Sietsma, Quantification of dislocation structures from anelastic deformation behaviour, Acta Mater. 115 (2016) 314–323.
[5] T. Ungár, J. Gubicza, P. Hanák, I. Alexandrov, Densities and character of dislocations and size-distribution of subgrains in deformed metals by X-ray diffraction profile analysis, Mater. Sci. Eng. A 319–321 (2001) 274–278.
[6] I. Groma, X-ray line broadening due to an inhomogeneous dislocation distribution, Phys. Rev. B 57 (1998) 7535–7542.
[7] G. Ribárik, T. Ungár, J. Gubicza, MWP-fit: a program for multiple whole-profile fitting of diffraction peak profiles by ab initio theoretical calculations, J. Appl. Cryst. 34 (2001) 669–676.
[8] T. Shintani, Y. Murata, Evaluation of the dislocation density and dislocation character in cold rolled Type 304 steel determined by profile analysis of X-ray diffraction, Acta Mater. 59 (2011) 4314–4322.
[9] F. HajyAkbary, J. Sietsma, A.J. Böttger, M.J. Santofimia, An improved X-ray diffraction analysis method to characterize dislocation density in lath martensitic structures, Mater. Sci. Eng. A 639 (2015) 208–218.
[10] L. Li, T. Ungár, Y.D. Wang, J.R. Morris, G. Tichy, J. Lendvai, Y.L. Yang, Y. Ren, H. Choo, P.K. Liaw, Microstructure evolution during cold rolling in a nanocrystalline Ni-Fe alloy determined by synchrotron X-ray diffraction, Acta Mater. 57 (2009) 4988–5000.
[11] T. Seymour, P. Frankel, L. Balogh, T. Ungár, S.P. Thompson, D. Jädernäs, J. Romero, L. Hallstadius, M.R. Daymond, G. Ribárik, M. Preuss, Evolution of dislocation structure in neutron irradiated Zircaloy-2 studied by synchroton X-ray peak profile analysis, Acta Mater. 126 (2017) 102–113.
[12] T. Narutani, J. Takamura, Grain-size strengthening in terms of dislocation density measured by resistivity, Acta Metall. Mater. 39 (1991) 2037–2049.
[13] B. Jakobsen, H.F. Poulsen, U. Lienert, J. Almer, S.D. Shastri, H.O. Sørensen, C. Gundlach, W. Pantleon, Formation and subdivision of deformation structures during plastic deformation, Science 312 (2006) 889–892.
[14] U. Messerschmidt, Dislocation Dynamics During Plastic Deformation, Springer Verlag, Berlin, 2010.
[15] (a) J.M. Burgers, Some considerations on the fields of stress connected with dislocations in a regular crystal lattice, Proc. R. Neth. Acad. Sci. 42 (1939) 293–395; (b) J.M. Burgers, Geometrical considerations concerning the structural irregularities to be assumed in a crystal, Proc. Phys. Soc. 52 (1940) 23–33.
[16] U.F. Kocks, Relation between polycrystal deformation and single-crystal deformation, Metall. Trans. 1 (1970) 1121–1143.
[17] P. van Liempt, J. Sietsma, A physically based yield criterion I. Determination of the yield stress based on analysis of pre-yield dislocation behaviour, Mater. Sci. Eng. A 662 (2016) 80–87.
[18] G. Schoeck, Dislocation theory of plasticity of metals, Adv. Appl. Mech. 4 (1956) 229–279.
[19] G.I. Taylor, The mechanism of plastic deformation of crystals, Part I: theoretical, Proc. R. Soc. A 145 (1934) 362–387.